Journal of the Serbian Chemical Society
JSCS-info@shd.org.rs • www.shd.org.rs/JSCS

ACCEPTED MANUSCRIPT

Journal of the Serbian Chemical Society
JSCS-info@shd.org.rs • www.shd.org.rs/JSCS
J. Serb. Chem. Soc. **00(0)** 1-18 (2026)
JSCS–13760
Original scientific paper
Published DD MM, 2026

Energetic networks of lone pair–π interactions in phycobiliprotein interfaces: structural organization, geometry, and cooperative stabilization

LUKA M. BREBERINA[1], MARIO V. ZLATOVIĆ[2], SRĐAN Đ. STOJANOVIĆ[3] AND MILAN R. NIKOLIĆ[1]*

[1]*University of Belgrade – Faculty of Chemistry, Department of Biochemistry, Belgrade, Serbia,* [2]*University of Belgrade – Faculty of Chemistry, Department of Organic Chemistry, Belgrade, Serbia, and* [3]*University of Belgrade, Institute of Chemistry, Technology and Metallurgy – National Institute of the Republic of Serbia, Department of Chemistry, Belgrade, Serbia.*

(Received 3 February; revised 13 March; accepted 30 March 2026)

Abstract: Lone pair–π interactions represent an underexplored class of noncovalent forces in protein architecture, despite their fundamental electronic significance. Here, we present a comprehensive computational and bioinformatics analysis of lone pair–π interactions at phycobiliprotein interfaces based on 20 high-resolution X-ray crystal structures. Using defined geometric criteria and *ab initio* quantum-chemical calculations at the LMP2/cc-pVTZ++ level on reduced molecular models, we systematically characterized their distribution, geometry, topology, and energetic contributions. We identified 2,245 lone pair–π interactions, revealing a highly nonrandom and chemically selective interaction landscape dominated by oxygen-based lone pair donors and aromatic π acceptors, particularly Tyr and Phe. Geometric analysis showed strong distance and angular preferences, consistent with directional donor–acceptor orbital interactions rather than nonspecific packing effects. Energy calculations revealed a structured interaction potential surface, with stabilizing energies clustering in the −0.1 to −5.0 kJ mol^{-1} range within defined geometric domains. Network analysis further demonstrated that more than half of the interactions participate in cooperative, furcated lone pair–π motifs, generating interfacial stabilization through multivalent interaction networks. Collectively, these results establish lone pair–π interactions as geometry-encoded, energetically selective, and cooperatively organized stabilizing elements that contribute to interfacial specificity, structural precision, and quaternary structure stability in phycobiliprotein assemblies.

Keywords: phycobiliproteins; lone pair–π; interfaces, interactions, *in silico* studies.

* Corresponding author. E-mail: mnikolic@chem.bg.ac.rs
https://doi.org/10.2298/JSC260230017B

INTRODUCTION

Noncovalent interactions provide the fundamental energetic framework that governs protein folding, molecular recognition, and the formation of stable protein–protein interfaces in supramolecular assemblies. Classical interaction types such as hydrogen bonds, salt bridges, hydrophobic interactions, and π–π stacking have long been recognized as central stabilizing forces in protein structure and protein–protein interfaces.[1,2] However, advances in quantum chemistry and structural bioinformatics have shown that protein stability and specificity are also influenced by a diverse range of weak but highly directional electronic interactions, including n→π*, cation–π, anion–π, and lone pair–π interactions.[3–5] Although individually modest in energy, these interactions can have significant structural effects through cooperativity, spatial organization, and network formation.

Lone pair–π interactions arise from the interaction between a heteroatom lone pair orbital (n) and an aromatic or conjugated π system. These interactions involve electrostatic attraction, dispersion forces, and partial orbital donation from the lone pair into antibonding π* orbitals.[5–7] Unlike n→π* interactions, which involve carbonyl antibonding orbitals, lone pair–π interactions involve aromatic π systems and therefore display distinct geometric preferences and interaction topologies. Quantum-mechanical studies have shown that these interactions are highly geometry-dependent, directional, and energetically structured, forming defined stabilization minima in configuration space rather than diffuse, nonspecific attraction.[8,9] Lone pair–π interactions can be systematically classified by the identity of the lone pair donor atom (O, N, S, halogen), the electronic nature of the interacting π system (aromatic hydrocarbons, heteroaromatics, conjugated systems, nucleobases), and the biological context in which they occur (protein–ligand binding, protein–protein interfaces, protein–nucleic acid recognition, and water-mediated networks).[9–11] This multidimensional classification framework enables structured identification, annotation, and functional interpretation of lone pair–π interactions across biomolecular systems (Fig. 1).

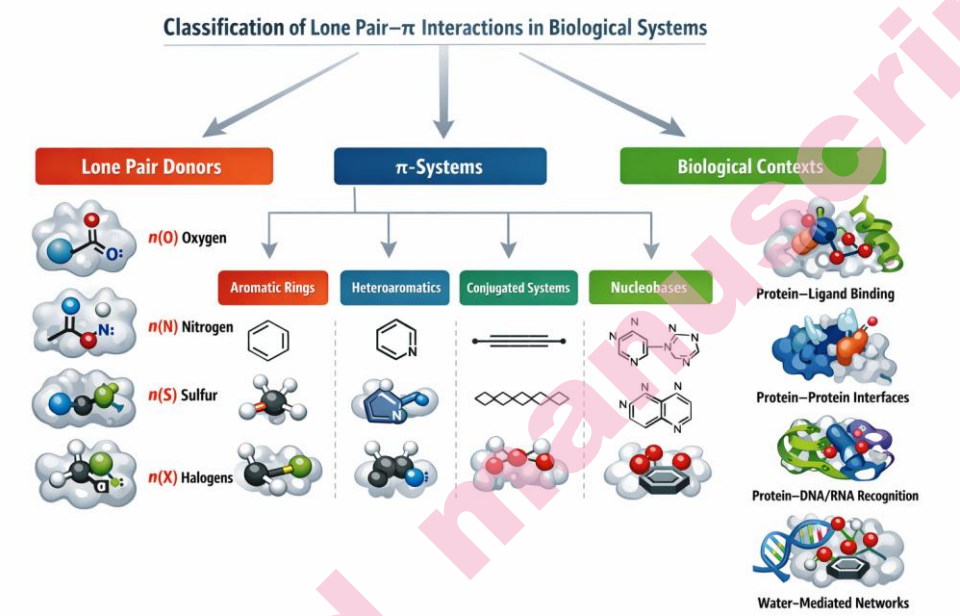

Fig. 1. Schematic representation of the multidimensional classification framework for lone pair–π interactions in biological systems. Lone pair–π interactions are organized along three orthogonal dimensions: 1) identity of the lone pair donor atom (oxygen, nitrogen, sulfur, halogens); 2) electronic nature of the interacting π-system (aromatic hydrocarbons, heteroaromatic systems, conjugated unsaturated systems, nucleobases); and 3) biological context (protein–ligand binding, protein–protein interfaces, protein–nucleic acid recognition, water-mediated interaction networks). This integrated classification highlights the structural diversity, mechanistic variability, and functional relevance of lone pair–π interactions in biomolecular systems.

Despite their well-established physical basis, lone pair–π interactions remain systematically underexplored in biological macromolecules, particularly at protein–protein interfaces.[2,12,13] Most structural analyses of protein complexes focus on hydrogen bonding, hydrophobic packing, and electrostatic complementarity, while orbital-driven interactions are rarely included in standard interaction classifications.[14,15] Consequently, the contribution of lone pair–π interactions to interface organization, specificity, and stability has not been quantitatively assessed at the proteome or structural family level.

Phycobiliproteins are an ideal model system for studying such interactions. These highly ordered, oligomeric light-harvesting proteins form stable supramolecular assemblies with dense packing, extensive interfacial contact surfaces, and precise chromophore–protein and protein–protein organization. Their quaternary structures depend on finely balanced noncovalent interaction networks that provide both structural stability and functional flexibility.[16] Although hydrogen bonds, salt bridges, and hydrophobic interactions in

phycobiliprotein assemblies have been extensively studied, the role of weak electronic interactions, such as lone pair–π interactions, remains largely unexplored.

In this study, we present a comprehensive structural, geometric, and energetic analysis of lone pair–π interactions at phycobiliprotein interfaces. Using a curated dataset of high-resolution X-ray crystal structures combined with ab initio quantum-chemical calculations, we characterize their distribution, preferred geometries, and energetic contributions. Beyond pairwise interactions, we introduce a network-based perspective showing that lone pair–π contacts frequently form multivalent motifs that contribute to the cooperative structural organization of protein interfaces.

By integrating structural bioinformatics, quantum chemistry, and energy landscape analysis, this study expands the current conceptual framework for protein interface stabilization and highlights lone pair–π interactions as an important yet previously underappreciated component of supramolecular protein organization. The aim of this study was to systematically characterize the structural organization, geometry, and energetic contributions of lone pair–π interactions at phycobiliprotein interfaces.

EXPERIMENTAL

Dataset

For this study, we used the PDB, accessed on November 10, 2025, which listed 247,081 resolved structures.[17] The selection criteria for including phycobiliproteins in the dataset were as follows: (a) structures of proteins containing the phycobiliprotein alpha or beta subunit domain (SCOP Classification, version 1.75)[18] were included; (b) theoretical models and NMR structures were excluded due to difficulties in assessing their accuracy compared to X-ray diffraction studies. Only crystal structures with a resolution of 2.0 Å or better and a crystallographic R-factor of 25.0% or lower were accepted; (c) only representatives with at least 30% sequence identity were included in the analyses.

After assembling the dataset, several structures containing ligands and mutant amino acids were excluded, leaving 20 phycobiliproteins in the dataset used for our bioinformatics analysis. Hydrogen atoms were added and optimized as needed using the program REDUCE[19] with its default settings. This software adds hydrogen atoms to macromolecule (protein and DNA) structures in standardized geometry, optimizing their orientations for OH, SH, $NH3^{+}$, Met methyls, Asn and Gln side-chain amides, and His rings. REDUCE selects the optimal hydrogen positions by choosing the overall best score from all possible combinations, considering individual scores assigned to each residue and groups containing movable protons partitioned into closed sets of local interacting networks.

The PDB IDs of all selected phycobiliprotein structures were as follows: 1all (Allophycocyanin (APC) from *Spirulina platensis*), 1b33 (APC from *Mastigocladus laminosus*), 1cpc (C-Phycocyanin (C-PC) from *Microchaete diplosiphon*), 1f99 (R-PC from *Polysiphonia urceolata*), 1gh0 (C-PC from *Arthrospira platensis*), 1jbo (C-PC from *Synechococcus elongatus*), 1kn1 (APC from *Neopyropia yezoensis*), 1phn (PC from *Cyanidium caldarium*), 2bv8 (PC from *Nostoc sp.* R76DM), 2vjt (APC from *Gloeobacter violaceus*), 2vml

(PC from Gloeobacter violaceus), 3dbj (APC from *Thermosynechococcus vulcanus*), 3o18 (C-PC from *Themosynechococcus vulcanus*), 4f0u (APC from *Synechococcus elongatus* PCC 7942), 4l1e (C-PC from *Leptolyngbya sp.* N62DM), 4lm6 (PC612 from *Hemiselmis virescens* M1635), 4lms (PC577 from *Hemiselmis pacifica* CCMP 706), 4po5 (APC from *Synechocystis* PCC 6803), 4rmp (APC from *Phormidium sp.* A09DM), and 4yjj (PC from *Phormidium rubidum*).

Lone pair–π interaction analysis

Protein structures containing various types of lone pair–π interactions were analyzed using Discovery Studio Visualizer 2025[20] with specific criteria and geometric feature settings. Lone pair–π interactions occur between a lone pair and a π ring if the following criteria are met (Fig. 2): 1) Hydrogen bond acceptor atoms are considered as long as they do not already participate in other atom–π ring interactions. 2) The distance between the acceptor and the ring centroid is within the π–lone pair (max dist) cutoff (7.0 Å). 3) The angle between the acceptor centroid vector and the normal to the ring plane is less than the π–lone pair angle (90°). Because lone pair orbitals cannot be directly observed in X-ray crystal structures, their orientation relative to the aromatic π system must be approximated using geometric criteria. In this study, the donor atom–centroid distance and the angle between the donor–centroid vector and the normal to the aromatic ring plane were used as geometric proxies to approximate the preferred directionality of the lone pair toward the π electron cloud.

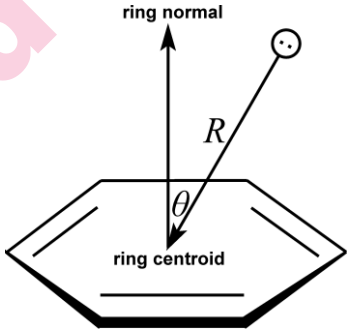

Fig. 2. Parameters for lone pair–π interactions: (*R*) the distance between the lone pair and the centroid; (*θ*) the angle between the lone pair–centroid vector and the normal to the ring plane.

Computation of lone pair–π interaction energy

To perform *ab initio* calculations to determine the energies of lone pair–π pairs at the desired level of theory, with adequate accuracy and within a satisfactory time frame, we used structurally reduced model systems.[21,22] Phenylalanine was simplified to methylbenzene 1), histidine to 5-methyl-1*H*-imidazole 2), and tryptophan and tyrosine were reduced to 3-methyl-1*H*-indole 3) and 4-methylphenol 4), respectively (Fig. 3).

Ab initio calculations were performed in a vacuum using Jaguar from Schrödinger Suite 2018-1[23], employing the LMP2 method with the triple zeta Dunning correlation-consistent basis set[24] and ++ diffuse functions[25]. The LMP2 method, used to study lone pair–π interactions, was significantly faster than the MP2 method. However, the calculated interaction energies and equilibrium distances from both methods are almost identical.[26] Several authors have found that LMP2 is an excellent method for calculating protein interaction energies.[27–29]

Geometries of interacting structures were optimized using the LMP2/cc-pVTZ(-f)++ level of theory, and their single-point energies were calculated at the LMP2/cc-pVTZ++ level. In practice, the optimized model fragments were first generated independently at the LMP2/cc-pVTZ(−f)++ level. The optimized fragments were then spatially aligned with the corresponding residues in the crystal structures by superimposing the heavy atoms of the model systems onto the atomic coordinates extracted from the protein structures. This procedure preserves the experimentally observed relative orientation of the interacting groups while using the optimized model geometries for reliable quantum-chemical energy evaluation. Frequency calculations were performed for all optimized model systems at the same level of theory to verify that the structures correspond to true minima on the potential energy surface. All optimized structures showed no imaginary frequencies.

Interaction energies were evaluated using a large correlation-consistent triple-ζ basis set with diffuse functions (cc-pVTZ++). Although basis set superposition error (BSSE) can influence very weak interactions, using an extended basis set substantially reduces this effect. Consequently, BSSE is expected to introduce only a small systematic shift in absolute energies without affecting the qualitative trends observed across the interaction dataset.

The lone pair–π interaction energies in dimers (lone pair–π pairs) were calculated as the difference between the energy of the complex and the sum of the energies of the monomers in their optimized geometries.

The nature of the aromatic π system also influences the interaction energy. Phenylalanine and tyrosine represent the dominant π acceptors in the analyzed dataset. While both provide similar aromatic π surfaces, the phenolic group of tyrosine introduces additional polarization and electrostatic effects that may slightly enhance lone pair–π stabilization compared with purely hydrocarbon aromatic systems such as phenylalanine. These electronic differences contribute to the observed distribution of interaction geometries and energies.

From the complete set of identified lone pair–π contacts, representative model dimers were constructed for quantum-chemical interaction energy calculations. The selected model systems preserve the experimentally observed geometry of the interacting fragments while allowing accurate evaluation of the interaction energies. Cartesian coordinates of the representative optimized dimers are provided in the Supplementary material.

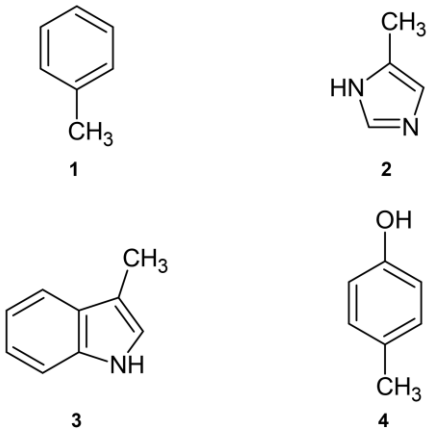

Fig. 3. Structurally simplified structures used for lone pair–π interaction energy calculations: 1) instead of Phe; 2) instead of His; 3) instead of Trp; 4) instead of Tyr.

RESULTS AND DISCUSSION

This manuscript examines the role of lone pair–π interactions at phycobiliprotein interfaces and their environmental preferences. We performed a computational analysis of 20 X-ray crystallographic structures of phycobiliproteins and summarized lone pair–π interactions to better understand the high stability of intrinsic phycobiliprotein oligomers. Furthermore, we analyzed the relative preference of lone pair–π interacting amino acids at interfaces, interaction geometries, and energetic contributions of lone pair–π interactions.

Distribution of lone pair–π interactions

Using the geometrical criteria defined in the Experimental section, we analyzed the frequency of aromatic amino acid residues involved in lone pair–π interactions. The results are shown in Table I. There are 2,245 lone pair–π interactions in phycobiliprotein interfaces in our dataset, with an average of 112 interactions per protein. This unexpectedly high interaction density indicates that lone pair–π contacts are not rare structural anomalies but are a systematic component of the noncovalent interaction landscape at phycobiliprotein interfaces.

TABLE I. Frequency of occurrence of lone pair–π interaction-forming residues at phycobiliprotein interfaces

Residue	Lone pair		π	
	Number[a]	Occurrence, %[b]	Number[a]	Occurrence, %[b]
Backbone	1197	53.3	-	-
Side-chain				
Asn	45	2.1	-	-
Asp	434	19.3	-	-
Gln	32	1.4	-	-
Glu	54	2.4	-	-
His	10	0.4	-	-
Met	37	1.7	-	-
Ser	113	5.0	-	-
Thr	176	7.8	-	-
Tyr	147	6.6	-	-
His	-	-	18	0.8
Phe	-	-	915	40.8
Trp	-	-	16	0.7
Tyr	-	-	1296	57.7
Total	2245	100	2245	100

[a] The number of times a particular amino acid occurs in an appropriate interaction; [b] The percentage of times the amino acid occurs in an appropriate interaction

The distribution of residues involved in lone pair–π interactions within phycobiliprotein interfaces is highly non-random and chemically selective, reflecting fundamental electronic and geometric principles that govern donor–

acceptor interactions between lone pair orbitals and aromatic π-electron systems. These interactions result from a combination of electrostatic attraction, orbital polarization, and dispersion forces, and are conceptually related to donor–acceptor frameworks described for n→π* interactions, while remaining mechanistically distinct because they involve aromatic π systems rather than carbonyl antibonding orbitals.[2,5,7,30] The data reveal a pronounced donor–acceptor asymmetry, with electron-rich, oxygen-containing groups acting primarily as lone pair donors and aromatic residues serving as the main π acceptors.

Backbone atoms are the primary source of lone pair donors (53.3%), highlighting the central role of peptide carbonyl oxygen atoms as universal and geometrically accessible lone pair contributors. Carbonyl oxygens are well-established participants in donor–acceptor orbital interactions in biological systems and are highly effective lone pair donors because of their strong electron density and favorable orbital orientation.[5,11] Their prevalence at protein interfaces underscores that lone pair–π interactions are intrinsic to protein architecture rather than dependent solely on side-chain chemistry.

Among side-chain contributors, oxygen-containing residues dominate the lone pair donor landscape, with Asp (19.3%), Thr (7.8%), Ser (5.0%), Tyr (6.6%), Glu (2.4%), and Asn (2.1%) accounting for most interactions. This distribution reflects the high electron density and favorable orbital orientation of oxygen lone pairs in carboxylate, carbonyl, and hydroxyl groups, which are optimal for lone pair–π coupling.[8,31] Carboxylate-containing residues (Asp, Glu) are particularly effective donors due to their delocalized negative charge and strong n-donor character, enabling robust electrostatic and polarization-driven interactions with π systems. Hydroxyl-bearing residues (Ser, Thr, Tyr) provide geometrically flexible lone pairs that can participate in directional lone pair–π interactions, often forming cooperative networks with hydrogen bonds and enhancing interface stability.[5,31] In this work, the term "cooperative" is used primarily in a structural and qualitative sense, referring to the spatial clustering of multiple lone pair–π contacts within protein interfaces. The analysis does not explicitly quantify energetic cooperativity through many-body energy decomposition but instead highlights the structural organization of interaction networks that may collectively contribute to stabilization.

In contrast, sulfur- and nitrogen-containing side chains contribute minimally to lone pair donation (Met 1.7%, His 0.4%), reflecting the lower energetic favorability, reduced directionality, and less optimal orbital overlap of sulfur and imidazole lone pairs in biological lone pair–π systems.[8] This selectivity indicates that lone pair–π interactions in proteins are chemically biased toward oxygen-based donors rather than representing a general lone pair phenomenon.

On the π-acceptor side, aromatic residues dominate the interaction landscape, with Tyr (57.7%) and Phe (40.8%) accounting for nearly all π contributions.

Aromatic rings are well-established π-electron acceptors in noncovalent interactions because of their delocalized electron clouds, quadrupole moments, and anisotropic electrostatic potentials.[4,7] Tyrosine plays a particularly central role, as its phenolic ring provides an efficient π-acceptor surface, while its hydroxyl group can serve as a lone pair donor in alternative geometries, enabling bidirectional lone pair–π connectivity and network formation within interfacial regions.[8,31]

The low contribution of tryptophan (0.7%), despite its extended π system, likely reflects steric constraints and structural burial of indole rings, which limit their accessibility for lone pair–π engagement at protein–protein interfaces. Similarly, histidine contributes minimally as a π acceptor because the heteroaromatic nature of the imidazole ring alters its π-electron density distribution and electrostatic surface compared to phenyl systems.[4]

We have also examined multiple lone pair–π interactions at phycobiliprotein interfaces. The analysis showed that about 56% of the dataset's lone pair–π interactions participate in multiple interactions. The presence of furcated lone pair networks at phycobiliprotein interfaces indicates that lone pair donors – primarily backbone carbonyl oxygens and polar side-chain oxygen atoms – and aromatic π-systems do not form isolated pairwise contacts, but instead create cooperative interaction clusters in which a single donor can engage multiple π-centers or a single π-system can accept multiple lone pair interactions. These topologies are consistent with cooperative donor–acceptor polarization and charge-redistribution models, where local electronic organization promotes network-like stabilization rather than discrete binary interactions.[3,32,33] Functionally, these furcated lone pair networks likely contribute to interfacial robustness and dynamic stability, enabling stabilization through distributed weak interactions rather than reliance on a small number of strong directional bonds.[5,34]

An illustrative example of multiple lone pair–π interactions is shown in Fig. 4. The interaction pattern observed in allophycocyanin from *Spirulina platensis* represents a structurally and electronically coherent case of furcated (multiple) lone pair–π interactions, in which a single residue acts as a multivalent donor to multiple aromatic π acceptors. The carboxylate group of A:Asp13 simultaneously engages both oxygen atoms (OD1 and OD2) in lone pair–π interactions with B:Tyr94 and B:Tyr97, generating a fourfold donor–acceptor network (OD1–Tyr94, OD1–Tyr97, OD2–Tyr94, OD2–Tyr97). This architecture reflects a bifurcated donor/multi-acceptor topology, where the delocalized lone pair electron density of the carboxylate group is distributed toward multiple π systems rather than forming a single localized interaction. At the electronic level, this motif is consistent with n→π* donation and electrostatically driven lone pair–π coupling, in which electron density from oxygen lone pair orbitals is transferred into low-lying antibonding π* orbitals of adjacent aromatic systems in a geometry-dependent and directional manner.[5,8] The simultaneous involvement of both OD1

and OD2 atoms indicates that the carboxylate group acts as a cooperative donor unit, enabling charge delocalization and interaction redundancy – a phenomenon analogous to cooperativity in hydrogen-bond networks but governed by orbital overlap and π-electron polarization rather than proton transfer.[35]

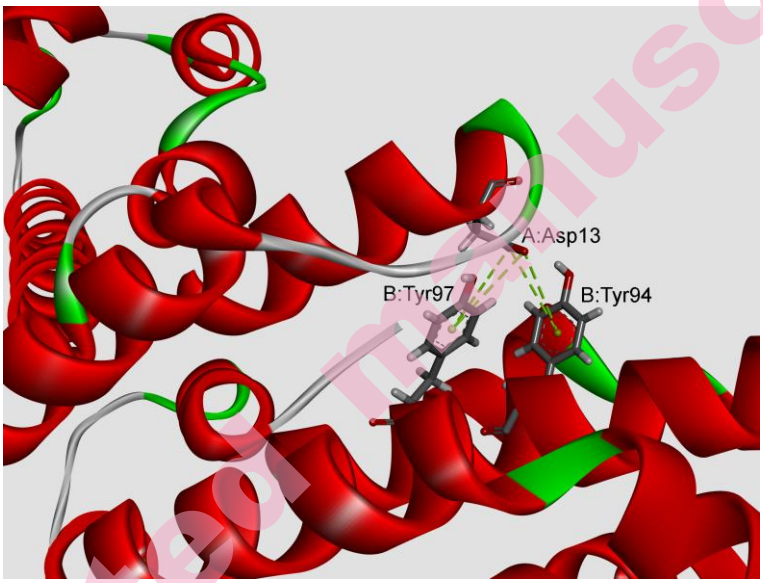

Fig. 4. Furcated (multiple) lone pair–π interaction network in allophycocyanin from *Spirulina platensis* (PDB ID: 1all). The carboxylate group of A:Asp13 simultaneously engages both oxygen atoms (OD1 and OD2) in lone pair–π interactions with two aromatic residues, B:Tyr94 and B:Tyr97, forming a fourfold interaction network: (1) A:Asp13:OD1–B:Tyr94, (2) A:Asp13:OD1–B:Tyr97, (3) A:Asp13:OD2–B:Tyr94, and (4) A:Asp13:OD2–B:Tyr97. This furcated lone pair–π motif reflects cooperative n→π* donation and multivalent electrostatic–orbital coupling, generating a stabilizing interaction network across the protein interface.[5,8]

Lone pair–π interactions in protein environments rarely occur in isolation. In many cases, additional noncovalent interactions, such as π–π stacking, CH–π contacts, and general dispersion interactions, also contribute to the stabilization of the observed structural motifs. Therefore, the lone pair–π contacts identified here should be considered components of a broader network of weak interactions that collectively contribute to interface stability. Such furcated lone pair–π networks transform intrinsically weak individual noncovalent interactions into collectively stabilizing motifs, enhancing interfacial robustness, restricting local conformational flexibility, and promoting precise aromatic alignment across protein–protein interfaces.[5,36] In phycobiliprotein assemblies, this multivalent lone pair–π architecture likely contributes to quaternary structure stabilization and electronic preorganization of the interface, supporting long-range structural

coherence and highlighting lone pair–π furcation as a previously underappreciated but mechanistically significant stabilizing principle in protein complexes.

Interaction geometries of lone pair–π interactions

The frequency distribution of the distance and angle parameters for lone pair–π interaction pairs is analyzed (Fig. 5).

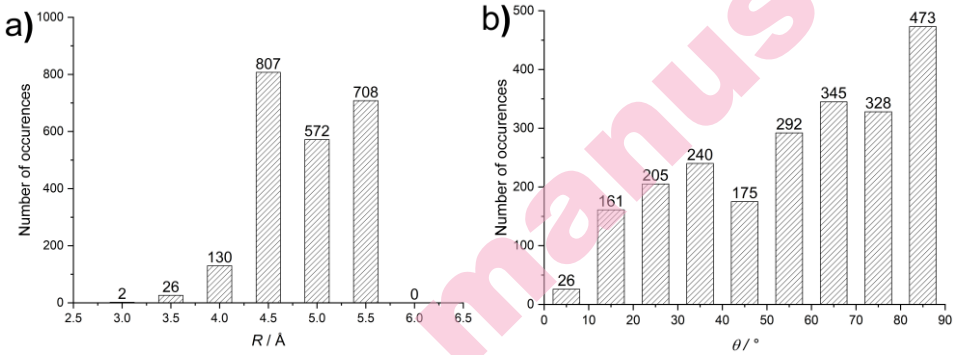

Fig. 5. Interaction geometries of lone pair–π interactions in phycobiliproteins: a) *R* distance distribution, b) θ angle distribution.

The R-distance distribution (Fig. 5a) shows a strong clustering of lone pair–π interactions in the 4.0–5.5 Å range, with clear maxima at 4.5 Å (807 occurrences) and 5.5 Å (708 occurrences), and a substantial population at 5.0 Å (572 occurrences). In contrast, very short distances (<3.5 Å) are extremely rare, and no interactions are observed beyond approximately 6.0 Å. This distance range is fully consistent with the established geometric window for stabilizing lone pair–π and n→π* interactions, which typically occur at donor–acceptor separations of approximately 3.0–5.5 Å, depending on the electronic nature of the donor atom and the π system involved.[5,35] Importantly, the dominance of mid-range distances suggests that these interactions in phycobiliprotein interfaces are not random contacts but electronically optimized noncovalent interactions, where electrostatic attraction and orbital overlap (lone pair → π* donation) operate in a balanced regime that maximizes stabilization while avoiding steric repulsion.[8,37]

The θ-angle distribution (Fig. 5b) further supports a directional and anisotropic interaction pattern, with a progressive enrichment toward larger angles and a pronounced maximum in the 80–90° bin (473 occurrences). This angular preference is highly characteristic of lone pair–π geometries, where the lone pair orbital approaches the aromatic π-cloud approximately perpendicular to the ring plane, optimizing electrostatic complementarity and orbital alignment (lone pair orbital → π* orbital interaction).[4,5] Such near-orthogonal approach geometries are inconsistent with purely nonspecific van der Waals contacts and instead reflect

orbital-controlled directionality, a hallmark of n→π* and lone pair–π interactions in biological systems.[5,8]

From a structural biology perspective, the combined distance–angle signature (R ≈ 4.0–5.5 Å, θ ≈ 60–90°) indicates that lone pair–π interactions in phycobiliprotein interfaces act as true structure-directing noncovalent interactions, comparable in geometric specificity to hydrogen bonds and π–π stacking, but governed by different electronic principles. Their enrichment at protein–protein interfaces supports the view that lone pair–π interactions contribute to interfacial complementarity, local stabilization, and interaction network formation, rather than representing incidental packing contacts.[5,8] The large number of interactions identified across independent crystal structures further supports the conclusion that lone pair–π contacts represent a recurrent, structurally encoded interaction type rather than incidental geometric contacts.

Taken together, these distributions demonstrate that lone pair–π interactions in phycobiliproteins are geometrically selective, directional, and electronically driven, supporting their classification as functionally relevant stabilizing interactions within supramolecular protein assemblies rather than as passive geometric coincidences.

Energetic contribution of lone pair–π interactions

Quantifying noncovalent interactions is essential for a rational approach to biological systems, including protein structure and function, antibody binding, drug design, and the development of supramolecular chemistry.[38] Therefore, the energetic contributions of residues involved in lone pair–π interactions were calculated using *ab initio* methods at the LMP2 level. The results for lone pair–π interacting pairs are shown in Fig. 6. To avoid calculating more than 2,000 interactions, we carefully selected 100 structures that represent nearly all of the interactions found.

Fig. 6 shows the three-dimensional energy–geometry landscape of lone pair–π interactions at phycobiliprotein interfaces, revealing a structured dependence of interaction energy on donor–π distance (R) and approach angle (θ). The three-dimensional energy–geometry landscape demonstrates that lone pair–π interactions at phycobiliprotein interfaces are governed by a well-defined energetic potential surface, rather than by a broad distribution of weak, nonspecific contacts. Energetically favorable interactions cluster within a narrow geometric domain defined by short donor–π distances (R ≈ 3.5–5.5 Å) and intermediate approach angles (θ ≈ 40–70°), corresponding to distinct local energy minima in the interaction landscape. The concentration of interaction energies in the range of approximately −0.1 to −5.0 kJ mol^{-1} indicates that lone pair–π contacts provide measurable and systematic stabilization, forming a reproducible energetic signature rather than stochastic low-energy fluctuations. This pattern reflects a structured stabilization mechanism, consistent with quantum-mechanical

descriptions of lone pair–π and n→π* interactions, which predict energy minimization through optimized orbital overlap and electrostatic complementarity rather than purely distance-dependent Coulombic attraction.[5,39]

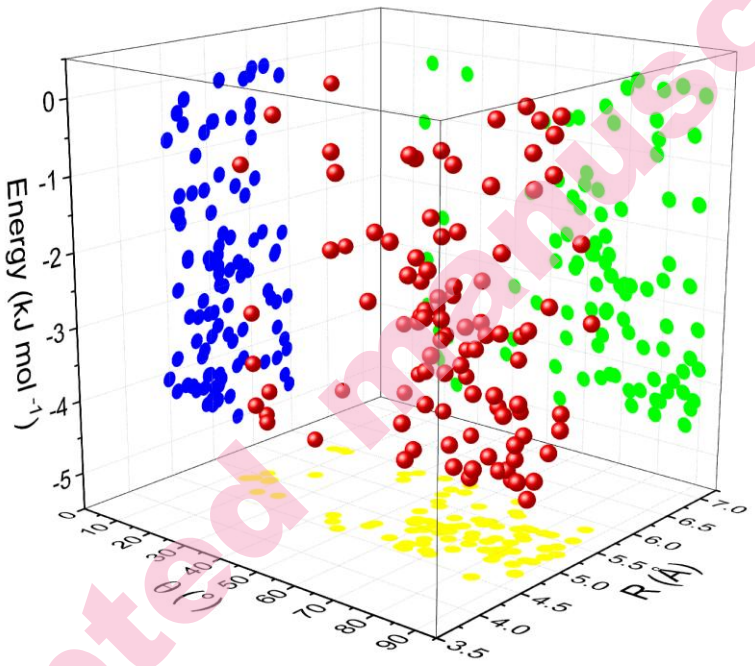

Fig. 6. 3D scatter plot from the energy analysis showing the distribution of energies depending on distance and angle for lone pair–π interacting pairs. A red circle denotes an energy that is an accepted lone pair–π interaction; yellow, green, and blue circles denote XY, XZ, and YZ projections, respectively.

Importantly, the energy distribution is highly anisotropic, showing strong stabilization only within restricted θ–R regions, indicating that lone pair–π interactions are governed by directional energetic constraints. The angular dependence of stabilization energy demonstrates that these interactions have a significant orbital delocalization component, where electron density transfer from heteroatom lone pairs into aromatic π* orbitals generates a directional energy minimum (n→π* stabilization), rather than an isotropic, dispersion-dominated attraction. This creates a discrete energetic well in configuration space, characteristic of weak but electronically structured noncovalent interactions.[5,8]

The systematic increase in interaction energy (reduced stabilization) at longer distances (R > 6.0 Å) and at extreme angular values (θ < 30° or > 80°) defines a steep energetic gradient away from the optimal stabilization zone, indicating rapid energetic decay outside the favorable interaction basin. This steep energy drop-off confirms the short-range energetic nature of lone pair–π interactions and rules out

interpretations based on long-range electrostatics or diffuse van der Waals stabilization. Energy decomposition models also predict that lone pair–π stabilization results from localized orbital interactions and therefore decays sharply with geometric displacement.[6,9]

Within phycobiliprotein interfaces, this energy landscape suggests that lone pair–π interactions serve as energetically selective stabilizing elements, contributing not through large individual interaction energies but through energetic cooperativity and accumulation. Multiple lone pair–π contacts, organized within optimal energetic domains, can collectively generate distributed stabilization energy, forming interfacial energy networks that enhance interface robustness, reduce local conformational entropy, and increase energetic barriers to dissociation. Thus, lone pair–π interactions act as fine-scale energetic modulators of protein–protein interfaces, refining stability and specificity through the spatial organization of multiple weak but energetically optimized interactions, directly analogous to cooperative hydrogen-bond and dispersion networks in structured protein interfaces.[5,8]

CONCLUSION

This study provides a systematic structural, geometric, and energetic characterization of lone pair–π interactions in phycobiliprotein interfaces, establishing them as functionally relevant noncovalent interactions rather than incidental packing contacts. Through large-scale structural analysis and ab initio quantum-chemical energy calculations, we show that lone pair–π interactions in phycobiliproteins are chemically selective, geometrically constrained, and energetically structured, forming reproducible stabilization patterns across protein–protein interfaces.

Our results show that lone pair–π interactions are primarily driven by oxygen-based lone pair donors and aromatic π acceptors, with specific distance and angular preferences that reflect directional donor–acceptor orbital coupling rather than diffuse electrostatic attraction. The computed energy landscape reveals discrete stabilization minima, indicating that lone pair–π interactions have intrinsic energetic organization, despite their individually modest interaction energies. Notably, the frequent occurrence of furcated and structurally cooperative lone pair–π motifs demonstrates that these interactions function as interfacial energy networks, where multiple weak contacts collectively generate distributed interaction networks that enhance interface robustness, reduce conformational entropy, and increase energetic barriers to dissociation.

In phycobiliprotein assemblies, this cooperative architecture positions lone pair–π interactions as fine-scale energetic modulators that complement hydrogen bonds, salt bridges, and hydrophobic interactions by providing geometric precision and electronic preorganization at protein–protein interfaces. More broadly, our

findings support a conceptual shift from viewing lone pair–π interactions as isolated weak contacts to recognizing them as organized, network-forming stabilizing elements that contribute to supramolecular protein structure and stability. The identification of over two thousand lone pair–π interactions in a relatively small dataset of phycobiliprotein structures highlights that these interactions are a widespread and previously underappreciated stabilizing component of protein–protein interfaces.

These results expand the current understanding of noncovalent interaction networks in proteins and highlight lone pair–π interactions as a previously underappreciated stabilizing principle in biological assemblies. The energetic network model presented here provides a new framework for interpreting weak orbital interactions at protein interfaces and offers a foundation for future studies of their roles in protein folding, oligomerization, molecular recognition, and biomolecular self-assembly.

SUPPLEMENTARY MATERIAL

Additional data are available electronically at the pages of journal website: https://www.shd-pub.org.rs/index.php/JSCS/article/view/13760, or from the corresponding author on request.

Acknowledgements: This research has been financially supported by the Ministry of Science, Technological Development, and Innovation of the Republic of Serbia (Contracts No: 451-03-136/2026-03/200026, and 451-03-33/2026-03/ 200168).

ИЗВОД

ЕНЕРГЕТСКЕ МРЕЖЕ LONE PAIR–π ИНТЕРАКЦИЈА У ИНТЕРФЕЈСИМА ФИКОБИЛИПРОТЕИНА: СТРУКТУРНА ОРГАНИЗАЦИЈА, ГЕОМЕТРИЈА И КООПЕРАТИВНА СТАБИЛИЗАЦИЈА

ЛУКА М. БРЕБЕРИНА[1], МАРИО В. ЗЛАТОВИЋ[2], СРЂАН Ђ. СТОЈАНОВИЋ[3] И МИЛАН Р. НИКОЛИЋ[1*]

[1]Универзитет у Београду, Хемијски факултет, Катедра за биохемију, Београд, Србија, [2]Универзитет у Београду, Хемијски факултет, Катедра за органску хемију, Београд, Србија, и [3]Универзитет у Београду, Институт за хемију, технологију и металургију, Центар за хемију, Институт од националног значаја за Републику Србију, Београд, Србија.

Lone pair–π интеракције представљају недовољно истражену класу нековалентних сила у архитектури протеина, упркос њиховом фундаменталном електронском значају. У овом раду представљамо свеобухватну рачунарску и биоинформатичку анализу lone pair–π интеракција у интерфејсима фикобилипротеина, засновану на 20 рендгенских кристалографских структура високе резолуције. Применом дефинисаних геометријских критеријума и *ab initio* квантно-хемијских прорачуна на LMP2/cc-pVTZ++ нивоу теорије на редукованим молекулским моделима, систематски смо окарактерисали њихову дистрибуцију, геометрију, топологију и енергетске доприносе. Идентификовано је укупно 2,245 lone pair–π интеракција, што указује на изразито неслучајан и хемијски селективан интеракциони пејзаж, којим доминирају донори lone pair електрона на бази кисеоника и ароматски π акцептори, нарочито тирозин и фенилаланин. Геометријска анализа показала

је изражене преференције у погледу дистанце и угла, у складу са усмереним донор–акцептор орбиталним интеракцијама, а не са неспецифичним ефектима паковања. Енергетски прорачуни открили су структурисану интеракциону потенцијалну површину, при чему се стабилизационе енергије групишу у опсегу од −0,1 to −5,0 kJ mol^{-1} унутар дефинисаних геометријских домена. Анализа мрежа додатно је показала да више од половине интеракција учествује у кооперативним, фуркованим lone pair–π мотивима, који генеришу стабилизацију интерфејса путем мултивалентних интеракционих мрежа. У целини, ови резултати успостављају lone pair–π интеракције као геометријски кодиране, енергетски селективне и кооперативно организоване стабилизационе елементе који доприносе интерфејсној специфичности, структурној прецизности и стабилности кватернарне структуре у фикобилипротеинским агрегатима.

(Примљено 2. фебруара; ревидирано 13. марта; прихваћено 30. марта 2026.)

REFERENCES

1. M. Konstantinidou, J. M. Virta, M. R. Arkin, *Acc. Chem. Res.* **58** (2025) 2840 (https://doi.org/10.1021/acs.accounts.5c00441)
2. P. Schake, S. N. Bolz, K. Linnemann, M. Schroeder, *Nucleic Acids Res*. **53** (2025) W463 (https://doi.org/10.1093/nar/gkaf361)
3. G. J. Bartlett, A. Choudhary, R. T. Raines, D. N. Woolfson, *Nat. Chem. Biol.* **6** (2010) 615 (https://doi.org/10.1038/nchembio.406)
4. D. A. Dougherty, *Acc. Chem. Res.* **46** (2013) 885 (https://doi.org/10.1021/ar300265y)
5. R. W. Newberry, R. T. Raines, *Acc. Chem. Res.* **50** (2017) 1838 (https://doi.org/10.1021/acs.accounts.7b00121)
6. I. V. Alabugin, M. Manoharan, S. Peabody, F. Weinhold, *J. Am. Chem. Soc.* **125** (2003) 5973 (https://doi.org/10.1021/ja034656e)
7. E. A. Meyer, R. K. Castellano, F. Diederich, *Angew. Chem. Int. Ed.* **42** (2003) 1210 (https://doi.org/10.1002/anie.200390319)
8. G. J. Bartlett, D. N. Woolfson, *Prot. Sci*. **25** (2016) 887 (https://doi.org/10.1002/pro.2896)
9. J. Novotny, S. Bazzi, R. Marek, J. Kozelka, *Phys. Chem. Chem. Phys.* **18** (2016) 19472 (https://doi.org/10.1039/C6CP01524G)
10. J. Kozelka, *Eur. Biophys. J*. **46** (2017) 729 (https://doi.org/10.1007/s00249-017-1210-1)
11. S. K. Singh, A. Das, *Phys. Chem. Chem. Phys.* **17** (2015) 9596 (https://doi.org/10.1039/C4CP05536E)
12. S. Jena, J. Dutta, K. D. Tulsiyan, A. K. Sahu, S. S. Choudhury, H. S. Biswal, *Chem. Soc. Rev.* **51** (2022) 4261 (https://doi.org/10.1039/D2CS00133K)
13. L. Hahn, T. Zorn, J. Kehrein, T. Kielholz, A. L. Ziegler, S. Forster, B. Sochor, E. S. Lisitsyna, N. A. Durandin, T. Laaksonen, V. Aseyev, C. Sotriffer, K. Saalwächter, M. Windbergs, A. C. Pöppler, R. Luxenhofer, *ACS Nano*. **17** (2023) 6932 (https://doi.org/10.1021/acsnano.3c00722)
14. L. Chen, X. Ruan, X. Li, H. Fu, *Comput. Mol. Biol.* **14** (2024) 182 (https://doi.org/10.5376/cmb.2024.14.0021)
15. Y. Yuan, C. Chen, X. Guo, B. Li, N. He, S. Wang, *Compr. Rev. Food Sci. Food Saf.* **23** (2024) e13285 (https://doi.org/10.1111/1541-4337.13285)

16. C. García-Gómez, D. E. Aguirre-Cavazos, A. Chávez-Montes, J. M. Ballesteros-Torres, A. A. Orozco-Flores, R. Reyna-Martínez, Á. D. Torres-Hernández, G. M. González-Meza, S. L. Castillo-Hernández, M. A. Gloria-Garza, M. Kačániová, M. Ireneusz-Kluz, J. H. Elizondo-Luevano, *Mar. Drugs*. **23** (2025) 201 (https://doi.org/10.3390/md23050201)
17. P. W. Rose, B. Beran, C. Bi, W. F. Bluhm, D. Dimitropoulos, D. S. Goodsell, A. Prlić, M. Quesada, G. B. Quinn, J. D. Westbrook, J. Young, B. Yukich, C. Zardecki, H. M. Berman, P. E. Bourne, *Nucleic Acids Res.* **39** (2011) D392-D401 (https://doi.org/10.1093/nar/gkq1021)
18. A. G. Murzin, S. E. Brenner, T. Hubbard, C. Chothia, *J. Mol. Biol.* **247** (1995) 536 (https://doi.org/10.1016/S0022-2836(05)80134-2)
19. J. M. Word, S. C. Lovell, J. S. Richardson, D. C. Richardson, *J. Mol. Biol*. **285** (1999) 1735 (https://doi.org/10.1006/jmbi.1998.2401)
20. Biovia, D.S. (2025) Discovery Studio Visualizer. San Diego.
21. V. R. Ribić, S. Đ. Stojanović, M. V. Zlatović, *Int. J. Biol. Macromol*. **106** (2018) 559 (https://doi.org/10.1016/j.ijbiomac.2017.08.050)
22. S. Đ. Stojanović, Z. Z. Petrović, M. V. Zlatović, *J. Serb. Chem. Soc*. **86**, (2021) 781 (https://doi.org/10.2298/JSC210321042S)
23. Schrödinger Release 2018-1: Jaguar, Schrödinger, LLC, New York, NY, 2018.
24. T. H. Dunning, Jr., *J. Chem. Phys*. **90** (1989) 1007 (https://doi.org/10.1063/1.456153)
25. T. Clark, J. Chandrasekhar, G. W. Spitznagel, P. V. R. Schleyer, *J. Comput. Chem.* **4** (1983) 294 (https://doi.org/10.1002/jcc.540040303)
26. A. D. Bochevarov, E. Harder, T. F. Hughes, J. R. Greenwood, D. A. Braden, D. M. Philipp, D. Rinaldo, M. D. Halls, J. Zhang, R. A. Friesner, *Int. J. Quantum Chem.* **113** (2013) 2110 (https://doi.org/10.1002/qua.24481)
27. G. J. Jones, A. Robertazzi, J. A. Platts, *J. Phys. Chem. B*. **117** (2013) 3315 (https://doi.org/10.1021/jp400345s)
28. K. E. Riley, J. A. Platts, J. Řezáč, P. Hobza, J. G. Hill, *J. Phys. Chem. A*. **116** (2012) 4159 (https://doi.org/10.1021/jp211997b)
29. E. Cukuroglu, A. Gursoy, O. Keskin, *Nucleic Acids Res*. **40** (2012) D829-D833 (https://doi.org/10.1093/nar/gkr929)
30. M. Egli, S. Sarkhel, *Acc. Chem. Res.* **40** (2007) 197 (https://doi.org/10.1021/ar068174u)
31. T. Steiner, *Angew. Chem. Int. Ed.* **41** (2002) 48 (https://doi.org/10.1002/1521-3773(20020104)41:1%3C48::AID-ANIE48%3E3.0.CO;2-U)
32. T. J. Mooibroek, P. Gamez, J. Reedijk, *CrystEngComm*. **10** (2008) 1501 (https://doi.org/10.1039/B812026A)
33. R. W. Newberry, G. J. Bartlett, B. VanVeller, D. N. Woolfson, R. T. Raines, *Prot. Sci.* **23** (2014) 284 (https://doi.org/10.1002/pro.2413)
34. V. A. Adhav, K. Saikrishnan, *ACS Omega* **8** (2023) 22268 (https://doi.org/10.1021/acsomega.3c00205)
35. H. B. Bürgi, J. D. Dunitz, J. M. Lehn, G. Wipff, *Tetrahedron* **30** (1974) 1563 (https://doi.org/10.1016/S0040-4020(01)90678-7)
36. L. M. Salonen, M. Ellermann, F. Diederich, *Angew. Chem. Int. Ed.* **50** (2011) 4808 (https://doi.org/10.1002/anie.201007560)
37. H. B. Bürgi, J. D. Dunitz, E. Shefter, *J. Am. Chem. Soc.* **95** (1973) 5065 (https://doi.org/10.1021/ja00796a058)

38. P. A. Maury, D. N. Reinhoudt, J. Huskens, *Curr. Opin. Colloid Interface Sci.* **13** (2008) 74 (https://doi.org/10.1016/j.cocis.2007.08.013)
39. H. B. Bürgi, *Inorg. Chem.* **12** (1973) 2321 (https://doi.org/10.1021/ic50128a021).